Syntheses and Antitumor Evaluation of *C(6)*-Isobutyl- and *C(6)*-Isobutenyl-Substituted Pyrimidines, and Dihydropyrrolo[1,2-*c*]pyrimidine-1,3-diones

by **Svjetlana Krištafor**[a]), **Tatjana Gazivoda Kraljević**[a]), **Simon M. Ametamey**[b]), **Mario Cetina**[c]), **Ivana Ratkaj**[d]), **Romana Tandara Haček**[c]), **Sandra Kraljević Pavelić**[d]), and **Silvana Raić-Malić***[a])

[a]) Department of Organic Chemistry, Faculty of Chemical Engineering and Technology, University of Zagreb, Marulićev trg 20, P.O. Box 177, HR-10000 Zagreb (phone: +385-1-4597213; fax: +385-1-4597224; e-mail: silvana.raic@fkit.hr)

[b]) Center for Radiopharmaceutical Sciences, ETH Zurich (Swiss Federal Institute of Technology), Wolfgang-Pauli-Strasse 10, CH-8093 Zurich

[c]) Department of Applied Chemistry, Faculty of Textile Technology, University of Zagreb, Prilaz baruna Filipovića 28a, HR-10000 Zagreb

[d]) Department of Biotechnology, University of Rijeka, Trg braće Mažuranića 10, HR-51000 Rijeka

[e]) Institute of Immunology, Rockefellerova 2, HR-10000 Zagreb

A growing body of evidence supports that pyrimidine derivatives, in which the sugar residues have been replaced by acyclic side chains, might be developed as promising anticancer agents that interfere with tumor cell proliferation, survival, and metastatic formation. In this work, we prepared novel pyrimidines bearing i-Bu (*i.e.*, **3**, **4**, and **7**–**9**) and isobutenyl (*i.e.*, **5** and **10**) side chains at C(6) and examined their *in vitro* effects on tumor cell lines. The dihydropyrrolo[1,2-*c*]pyrimidine-1,3-diones **6** and **11** were obtained as products of intramolecular cyclization, which occurred during the removal of Bn in **5** or MeO protecting groups in **10**. Fluorination of **3** with diethylaminosulfur trifluoride (DAST) and then dehydrohalogenation of the resulting fluorinated derivative **4** afforded 6-isobut-2′-enyl pyrimidine derivative **5** with a C(2′)=C(3′) bond. For the preparation of 6-isobut-1′-en-1-yl pyrimidine **10**, a synthetic strategy involving acetylation of the 1,3-diols was applied. Antitumor evaluation of compounds **3**–**11** showed that 2,4-dimethoxypyrimidine containing 6-[(1,3-dibenzyloxy)-2-hydroxy]methyl side chain, **3**, exerted a strong antiproliferative effect on the studied tumor cell lines. Additionally, it was shown that the mechanism of antiproliferative effect of **3** in HeLa cells include early G2/M arrest and apoptosis, as well as a p53-independent S-phase arrest upon prolonged treatment.

Introduction. – Pyrimidines are biologically important molecules and valuable heterocyclic nuclei for the design of pharmaceutical agents [1][2]. Pyrimidine nucleoside analogs are widely used as chemotherapeutic agents in the treatment of cancer [3–6]. In particular, the pyrimidine analog 5-fluorouracil (5-FU) is one of the most widely used drugs for the treatment of breast, gastrointestinal, and liver carcinoma [7]. Furthermore, carmofur is a 5-FU derivative that bears a potentiated antitumor activity, while at the same time being clinically less toxic [8][9]. In anticancer treatment regimens, pyrimidine nucleoside analogs are widely used in combinational chemotherapy. These compounds, mainly due to their DNA-damaging properties that cause arrest of cells in the S phase, are suitable for combinational treatments with other cell-cycle inhibitors targeting different signalling pathways. Such approach might enhance cytotoxicity of drugs and improve clinical response of patients [10]. Moreover, pyrrolo-pyrimidines have been attracting considerable attention in a view of the high

biological activity of these bicyclic compounds [11]. The excellent biological activities exhibited by *C(5)*- and/or *C(6)*-substituted uracil derivatives provide a good rationale for further exploration of chemistry and antitumoral activities of these pyrimidines [12–19].

In addition, we have reported that fluorinated pyrimidine derivatives containing the 3,3,3-trifluoro-2-hydroxyprop-1-enyl side chain at C(6) exhibited a pronounced effect against breast carcinoma (MCF-7), while the compound with the 2-(fluoromethyl)-2-acetoxypropyl chain exhibited moderate effect against cervical carcinoma (HeLa) [20]. *C(6)*-Substituted pyrimidines containing the 4-fluorophenyl moiety in the side chain showed pronounced antiproliferative effect on colon (SW620 and HCT116) and lung carcinoma (H460) [21]. The 6-(bromomethyl)-substituted pyrimidine derivatives showed marked cytotoxic activity against all evaluated tumor cell lines, particularly against colon carcinoma (SW620) [22].

Besides, findings from the molecular docking of some *C(6)*-substituted pyrimidines into the active site of *Herpes simplex* virus type 1 thymidine kinase (HSV-1 TK) indicated that these compounds showed the same interactions known for natural substrate thymidine [23][24]. Biological phosphorylation-pattern assays revealed that 6-(2,3-dihydroxypropyl)pyrimidine, 6-[3-hydroxy-2-(hydroxymethyl)propyl]pyrimidine, and its *N*-Me analog represent promising precursors of nontoxic reporter probes for the monitoring of HSV-1 TK gene expression by means of positron-emission tomography (PET) [23][25].

Taking into account the pharmacological potential of the cited class of compounds, we performed the presented study with the primary aim to evaluate the cytostatic potencies of pyrimidine derivatives bearing 6-isobutyl (in **3**, **4**, and **7**–**9**), and isobutenyl (in **5** and **10**) side chain, in addition to structurally related bicyclic compounds **6** and **11**. Moreover, among the tested compounds, **3** exerted a strong antiproliferative effect, and the mechanisms underlying this property were studied in further details on HeLa cells.

Results and Discussion. – 1. *Chemistry.* The syntheses of the *C(6)*-substituted pyrimidine derivatives were performed as indicated in *Schemes 1* and *2*. Pyrimidine derivative **1** was synthesized in analogy to [23], and ketone **2** was prepared using a modified *Corey–Kim* oxidation [26] of 1,3-bis(benzyloxy)propan-2-ol [27] with *N*-chlorosuccinimide (NCS) and Me_2S. The treatment of 2,4-dimethoxy-5,6-dimethylpyrimidine (**1**) with lithium diisopropylamide (LDA) in THF at $-55°$ afforded the lithiated pyrimidine precursor of **1**, which reacted *in situ* with ketone **2** to give pyrimidine derivative **3** [28] (*Scheme 1*).

To obtain the unsaturated side chain at C(6) of the pyrimidine derivative **I**, dehydration of tertiary alcohol **3** was attempted. The reaction of **3** with H_2SO_4 (20% (*v*/*v*)) did not yield the expected product with the isobutenyl side chain at C(6). Therefore, compound **3** was converted into its fluorinated analog **4** using diethylaminosulfur trifluoride (DAST) albeit in 20% yield (*Scheme 1*). In addition, compound **5**, derived from dehydrohalogenation of **4**, was obtained in 10% yield. Subsequently, **4** was treated with an excess of MeONa to afford the unsaturated pyrimidine derivative **5** in 75% yield. The presence of the C(2′)=C(3′) bond in **5** was deduced from the pattern

Scheme 1

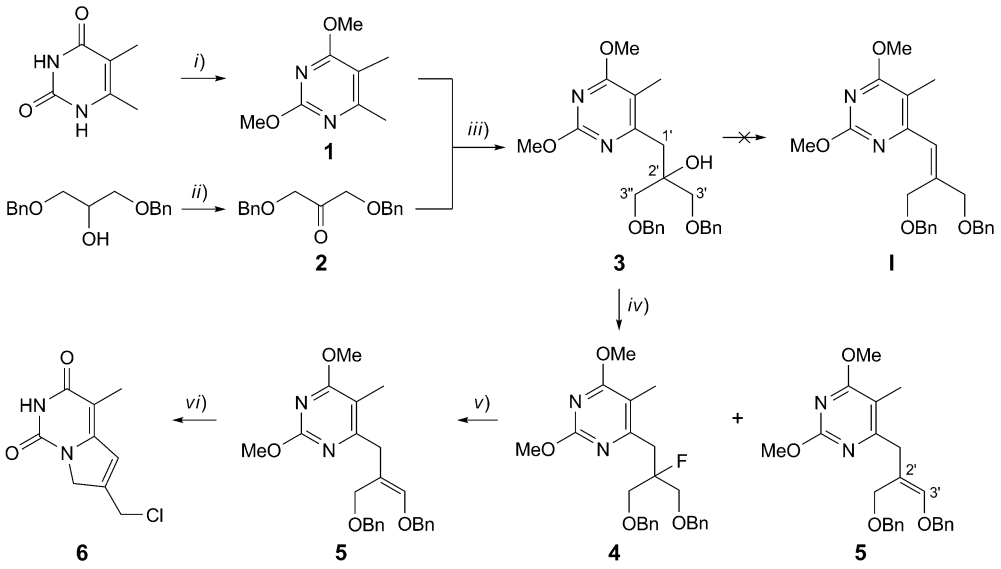

i) 1. $POCl_3$, reflux; 2. MeONa/MeOH, reflux. *ii*) *N*-Chlorosuccinimide (NCS), CH_2Cl_2, Me_2S, r.t. *iii*) Lithium diisopropylamide (LDA), THF, reagent **2**, $-55°$. *iv*) Diethylaminosulfur trifluoride (DAST), CH_2Cl_2, $-40°$. *v*) MeONa/MeOH. *vi*) BCl_3, CH_2Cl_2, $-40°$.

of chemical shifts, and on the basis of the magnitude and multiplicity of H,H spin-spin coupling constants (*cf. Exper. Part*).

The methylene groups $CH_2(1')$ and $CH_2(3'')$ in **5** display *singlet*s in the ^{1}H-NMR spectrum, while the corresponding CH_2 groups in **4** show *doublet*s caused by H,F coupling. Besides, the vinyl H-atom (H–C(3′)) in **5** is deshielded and appears as a *singlet*. Moreover, the CH_2 H-atoms ($PhCH_2O$) of the two Bn moieties in **5** display two signals due to chemical non-equivalency. On the contrary, corresponding H-atoms ($PhCH_2O$) in benzylated pyrimidine derivatives **3** and **4** are equivalent, and each exhibits one *singlet*. The removal of the Bn protecting groups in **5** was accomplished using BCl_3 at $-40°$ but was accompanied by an intramolecular cyclization and allylic rearrangement, which resulted in the formation of the bicyclic chloromethyl compound **6** (*Scheme 1*). The formation of **6** may be explained by the nucleophilic attack of N(1) at C(3″) of the chlorinated side chain at C(6). The structure of **6** was confirmed by X-ray crystallographic analysis.

The strategy for the preparation of 6-isobut-1′-enyl, instead of 6-isobut-2′-enyl pyrimidine derivatives, involved isopropylidene ketal formation as the most commonly used protection for 1,3-diols. However, in the attempted synthesis of the acetonide of **7** using acetone and AcCl, a mixture of 1,2- and 1,3-acetonides was obtained, in which the 1,2-acetonide was favored over the 1,3-derivative. An alternative route to obtain 6-isobut-1′-enyl pyrimidine derivative with 1,3-diols protected as acetates was then used as depicted in *Scheme 2*.

Scheme 2

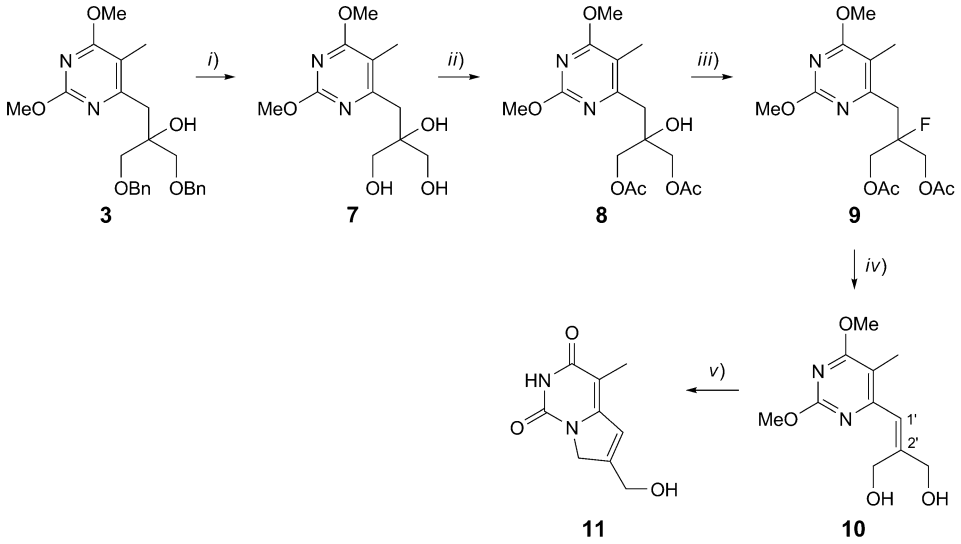

i) BCl_3, CH_2Cl_2, $-40°$. *ii*) Ac_2O; 4-(Dimethylamino)pyridine (DMAP), pyridine, MeCN, r.t. *iii*) Diethylaminosulfur trifluoride (DAST), CH_2Cl_2, $-40°$. *iv*) MeONa/MeOH. *v*) Me_3SiCl (TMSCl), NaI, MeCN, r.t.

Removal of the Bn groups was accomplished with BCl_3 to afford triol **7** in 70% yield. Conversion of the primary OH groups in **7** to ester functionalities was accomplished using Ac_2O and 4-(dimethylamino)pyridine (DMAP) to yield compound **8** with a free tertiary OH group. Treatment of **8** with DAST gave the fluorinated derivative **9**, which was then submitted to dehydrohalogenation with MeONa. The desired unsaturated pyrimidine derivative **10** with a C(1′)=C(2′) bond was obtained in 42% yield. The *C(6)*-side-chain H,H coupling patterns in ^{1}H-NMR spectra for **10** are *doublet*s corresponding to CH_2(3′) and CH_2(3″), *triplet*s for OH groups, and a *singlet* for H–C(1′).

Demethoxylation [29] of **10** using trimethylsilyl iodide (TMSI) provided bicyclic compound **11** in 67% yield. Intramolecular cyclization may be explained by nucleophilic attack of N(1) at C(3′) of the iodinated isobutenyl side chain.

2. *X-Ray Crystal Structure Study.* The structures of *C(6)*-substituted pyrimidine **3** and bicyclic compound **6** were unequivocally confirmed by single-crystal X-ray diffraction method. Compound **3** (*Fig. 1*) crystallizes with two independent molecules in the asymmetric unit in the orthorhombic space group *Pca*2_1. These two independent molecules, denoted as A and B, differ in the conformation of one of two $BnOCH_2$ groups, and thus, C(20) in molecule A is synclinal, whereas in molecule B is antiperiplanar with respect to C(22) of the Ph ring (C(20A)–O(5A)–C(21A)–C(22A), 62.7(5)°; C(20B)–O(5B)–C(21B)–C(22B), 172.1(4)°). Furthermore, C(10) is antiperiplanar in A and synclinal in B with respect to O(5) (C(10A)–C(11A)–C(20A)–O(5A), 179.2(4)°; C(10B)–C(11B)–C(20B)–O(5B), −54.7(5)°). The orientation of two Ph rings towards the pyrimidine ring is almost equal in molecule A. The

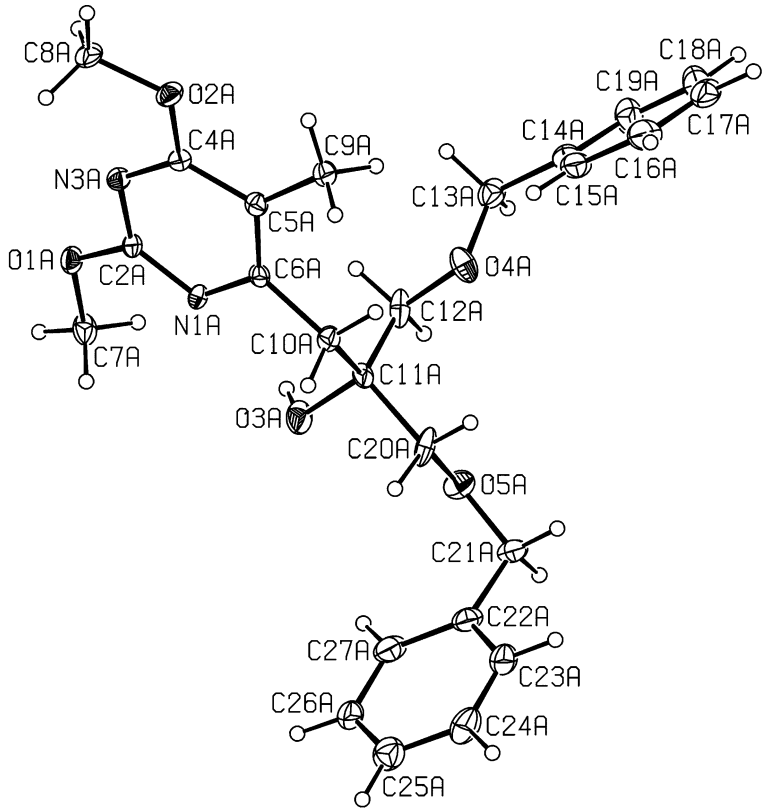

Fig. 1. *Molecular structure of* **3***, with the atom-numbering scheme.* For clarity, only one independent molecule is shown. Displacement ellipsoids for non-H-atoms are drawn at the 30% probability level.

dihedral angles between mean planes of the pyrimidine ring and Ph rings, C(14)–C(19) and C(22)–C(27), are 79.5(2) and 73.7(2)°, respectively. On the other hand, the orientation of the Ph rings in molecule B is slightly different, with the corresponding dihedral angles being 82.7(2) and 65.0(2)°, respectively. The bond lengths in 2,4-dimethoxypyrimidine are within the values of the equivalent ones in similar structures we published recently [30][31]. It should be pointed out that the C(4)–C(5) bond in 2,4-dimethoxy-6-(3,3,4,4,4-pentafluoro-2-hydroxybut-1-en-1-yl)pyrimidine [22] is *ca.* 0.04 Å shorter compared to all other structures.

Two intermolecular H-bonds, C(16B)···O(2A) and C(7B)···O(5A) (*Table 1*), join two independent molecules of **3**, so forming finite $D(2)$ motifs [32]. The H-donor atoms are exclusively atoms of molecule B, whereas the O-atoms of molecule A are exclusively H-acceptors. The combination of these two C–H···O H-bonds generates infinite chains (*Fig. 2*).

The supramolecular aggregation is augmented by aromatic $\pi\cdots\pi$ stacking interactions. The pyrimidine rings of the two independent molecules are mutually parallel (*Fig. 3*), with an interplanar angle of 0.75°, an interplanar spacing of 3.35 Å and 3.36 Å, and a corresponding centroid–centroid offset of 1.18 Å and 1.20 Å. Five

Table 1. *Intermolecular H-Bonding Geometries for* **3** *and* **6**

	D–H···A	D–H [Å]	H···A [Å]	D···A [Å]	D–H···A [°]	Symmetry codes
3	C(16B)–H(16B)···O(2A)	0.95	2.58	3.481(7)	158	$x, y, 1+z$
	C(7B)–H(72B)···O(5A)	0.98	2.47	3.384(6)	155	$x, -1+y, z$
6	N(3)–H(3)···O(2)	0.80(2)	2.01(2)	2.807(3)	171(2)	$3-x, 1-y, 1-z$
	C(10)–H(10B)···O(1)	0.97	2.54	3.332(3)	139	$2-x, ½+y, 1/2-z$
	C(11)–H(11B)···O(1)	0.97	2.54	3.356(3)	141	$2-x, ½+y, 1/2-z$

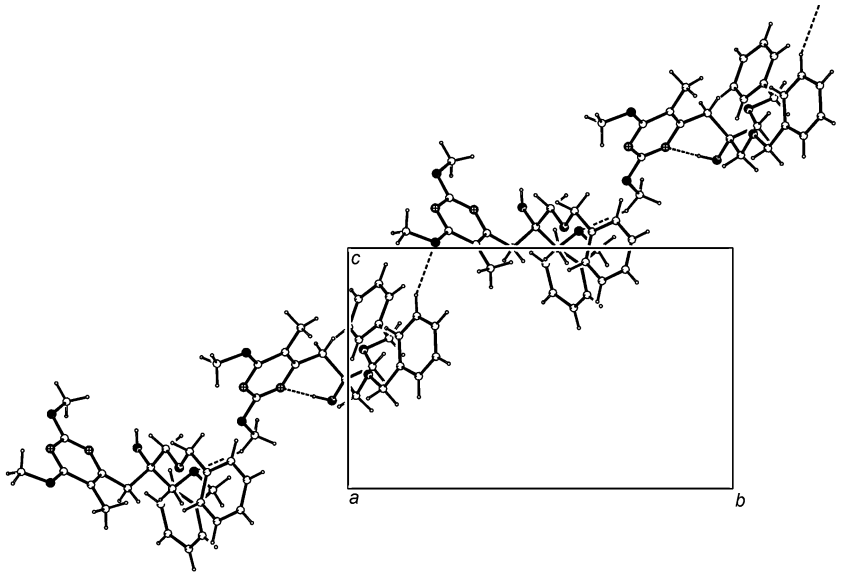

Fig. 2. *Crystal packing diagram of* **3***, viewed along the* a *axis, showing an infinite chain formed by two C–H···O H-bonds.* H-Bonds are indicated with dashed lines.

C–H···π interactions participate also in supramolecular aggregation of **3**. The H···Centroid (*Cg*) distances range from 2.63 to 3.00 Å, and C–H···*Cg* angles from 153° to 175°. The $\pi\cdots\pi$ and C–H···π interactions complete the three-dimensional framework.

In bicyclic compound **6** (*Fig. 4*), in which the six-membered and five-membered rings are linked *via* C(6) and N(1), crystallizes in the monoclinic space group $P2_1/c$. These two rings are nearly parallel, as the dihedral angle between their mean planes is 0.30(10)°. The $ClCH_2$ group is in the plane of the five-membered ring, defined by the C(8)–C(9)–C(11)–Cl(1) torsion angle of 3.7(3)°. A survey of *Cambridge Structural Database* [33] revealed that this is the first structure in which at least one of three non-common ring C-atoms of the five-membered ring (C(8), C(9), or C(10)) is not sp^3-hybridized. Thus, the C(8) and C(9) are sp^2-hybridized, and the C(8)–C(9) bond of 1.343(3) Å has a character of a C_{sp^2}=C_{sp^2} bond.

The molecules of **6** are linked by N(3)···O(2) H–bonds (*Table 1* and *Fig. 5*) into centrosymmetric dimers *via* eight-membered rings. This characteristic motif for

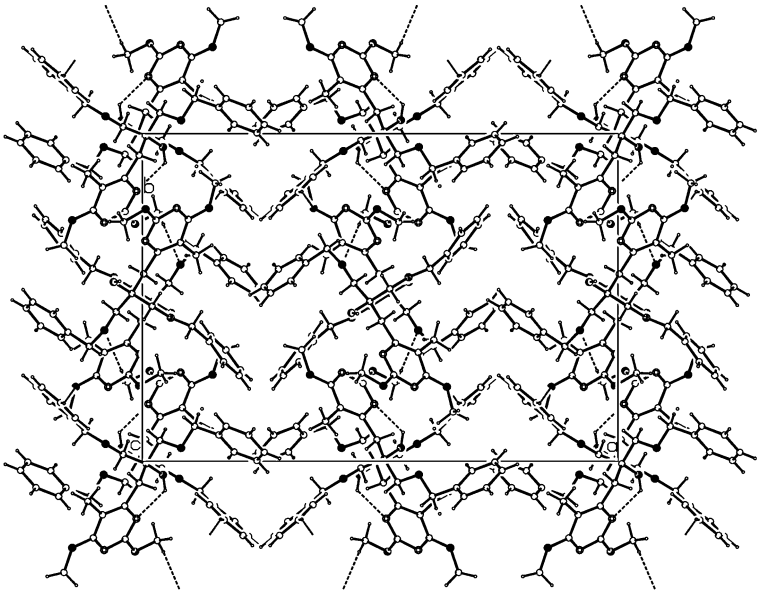

Fig. 3. *Crystal packing diagram of* **3***, viewed along the* c *axis, showing the packing of the molecules.* H-Bonds are indicated with dashed lines.

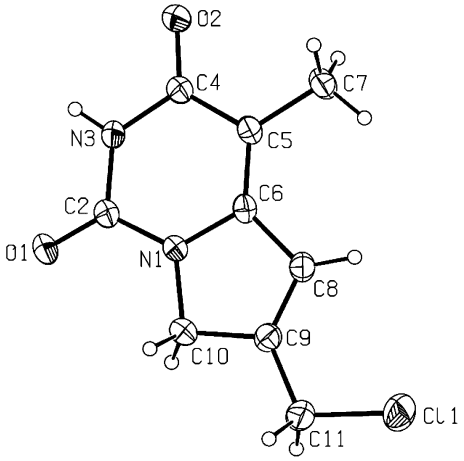

Fig. 4. *Molecular structure of* **6***, with the atom-numbering scheme.* Displacement ellipsoids for non-H-atoms are drawn at the 30% probability level.

pyrimidine derivatives can be defined by a graph-set notation as $R_2^2(8)$. In addition, two C–H···O H-bonds form $R_2^1(6)$ ring, so forming a three-dimensional network.

3. *Antitumor Activities.* Compounds **3**–**11** were evaluated for their cytostatic activities against human malignant tumor cell lines: cervical carcinoma (HeLa), breast epithelial adenocarcinoma, metastatic (MCF-7), hepatocellular carcinoma (HepG2), colorectal adenocarcinoma (SW620), pancreatic carcinoma (MiaPaCa-2), and normal

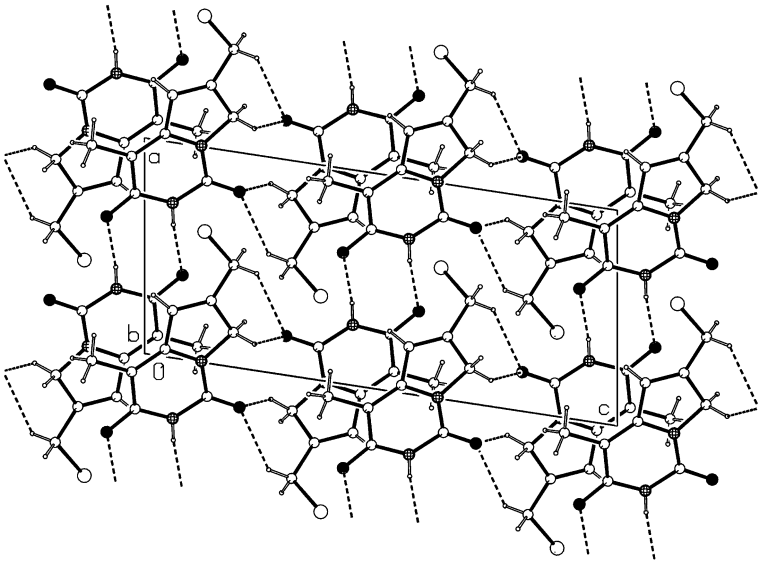

Fig. 5. *Crystal packing diagram of* **6**, *viewed along the* b *axis, showing N–H···O and C–H···O H-bonds.* H-Bonds are indicated with dashed lines.

human fibroblasts (WI38) (*Table 2*). Their effects were compared to antiproliferative activity of a compound regularly used for chemotherapy of cancer patients, 5-fluorouracil (5-FU). Among all synthesized compounds, only 2,4-dimethoxypyrimidine with 6-[(1,3-dibenzyloxy)-2-hydroxy]methyl side chain, **3**, showed a prominent concentration-dependent inhibitory activity similar to those obtained by 5-FU against all tested cell lines. Similarly to 5-FU, compound **3** exhibited also a cytostatic activity

Table 2. *Inhibitory Effects of* C(6)*-Substituted Pyrimidine Derivatives* **3**–**11** *and 5-Fluorouracil* (5-FU) *as Control Compound on the Growth of Malignant Tumor Cell Lines and Normal Fibroblasts*

	IC_{50} [μM][a])					
	HeLa	MCF-7	HepG2	SW620	MiaPaCa-2	WI38
3	3.67 ± 0.45	4.22 ± 0.43	2.42 ± 0.69	3.48 ± 0.9	6.08 ± 0.37	3.84 ± 0.39
4	> 100	> 100	> 100	> 100	> 100	> 100
5	> 100	85.15 ± 0.13	48.02 ± 0.23	64.61 ± 0.36	67.81 ± 0.35	78.78 ± 0.16
6	> 100	> 100	94.6 ± 0.16	> 100	> 100	> 100
7	> 100	> 100	> 100	> 100	> 100	> 100
8	> 100	> 100	> 100	> 100	> 100	> 100
9	95.89 ± 0.13	> 100	> 100	> 100	> 100	> 100
10	> 100	> 100	> 100	> 100	> 100	> 100
11	> 100	> 100	> 100	> 100	> 100	> 100
5-FU	4.4 ± 1.5	42.14 ± 11.43	8 ± 1.7	3.38 ± 2.49	11.45 ± 6.5	18.5 ± 17.1

[a]) IC_{50}; 50% Inhibitory concentration, or compound concentration required to inhibit tumor cell proliferation by 50%.

(IC_{50} 3.84 μM) against normal human fibroblasts (WI38). The pyrimidine derivative **5** bearing *C(6)*-isobutenyl side chain with the C(2′)=C(3′) bond showed moderate cytostatic activity against HepG2, MCF-7, SW620, MiaPaCa-2, and WI38 cell lines at the highest tested concentrations (IC_{50} ranging from 48.02 to 85.15 μM) (*Table 2*). In contrast, compounds **4**, **7**, **8**, **10**, and **11** did not exhibit any inhibitory effects. Due to the obtained results, compound **3**, bearing two benzylated and one free OH group in the *C(6)*-side chain, was chosen for further biological evaluation on HeLa cells that have the inactivated p53 protein [34]. It has been widely documented that many tumors bearing inactivated p53 protein and/or mutated p53 gene do not react well on therapy with common chemotherapeutic agents such as 5-FU [35][36]. Thus, we were interested in elucidation of the mechanism of antiproliferative effect on HeLa cells exerted by compound **3** in comparison to 5-FU. It is well-known that the main tumor suppressor activity of the functional gene p53 involves activation of the G1 cell-cycle checkpoint and/or apoptosis [37][38]. The results obtained by flow cytometric analysis of HeLa cells treated with compound **3** revealed a strong influence on the cell cycle, expectedly not involving a rise in G1 cell population (*Table 3*). After the 24-h treatment with compound **3**, an increase of cells in G2/M phase (12.8%) has been observed at a concentration of 1×10^{-5} M, as well as an increase of cells in subG1 (11.7%) at a concentration of 5×10^{-5} M, indicative for apoptosis. Interestingly, the main antiproliferative mechanism for compound **3** might be linked with the cell-cycle arrest in the S phase (ranging from 10.2–33.7%) observed upon the 48-h treatment at all tested concentrations accompanied with a concomitant decrease in G1 and subG1 cell populations. A similar effect was observed for HeLa cells treated with 5-FU (*Table 3*).

Table 3. *Flow Cytometric Analysis of HeLa Cells upon the 24 h and 48 h Treatments with Compound* **3** *and 5-FU*

		Cell percentage ([%] ± standard deviation)			
		subG1	G1	S	G2/M
3	Control 24 h	45.1 ± 2.3	59.9 ± 3.4	25.7 ± 4.9	14.4 ± 3.7
	5×10^{-6} M 24 h	43.2 ± 2.1	47.3 ± 5.4	30.5 ± 4.1	22.2 ± 4.8
	1×10^{-5} M 24 h	50.4 ± 2.7	52.7 ± 1.4	20.1 ± 2.8	27.2 ± 1.4[a])
	5×10^{-5} M 24 h	56.8 ± 0.7[a])	61.2 ± 1.1	19.4 ± 1.5	19.5 ± 2.5
	Control 48 h	53.6 ± 1.5	61.9 ± 4.2	21.9 ± 2.3	16.2 ± 2.6
	5×10^{-6} M 48 h	49.8 ± 0.7[a])	52.9 ± 1.3[a])	32.1 ± 2.9[a])	15.1 ± 2.3
	1×10^{-5} M 48 h	39.9 ± 1.1[a])	32.6 ± 4.8[a])	49.7 ± 4.1[a])	17.8 ± 0.7
	5×10^{-5} M 48 h	21.6 ± 0.8[a])	23.9 ± 4.1[a])	55.6 ± 3.2[a])	20.5 ± 4.3
5-FU	Control 24 h	6.96 ± 1.28	56.67 ± 1	30.7 ± 0.89	6.69 ± 1.28
	5×10^{-5} M 24 h	9.35 ± 0.51[a])	40.7 ± 0.68[a])	53.27 ± 1.42[a])	6.00 ± 0.35[a])
	1×10^{-6} M 24 h	7.96 ± 0.59	55.1 ± 1.31	32.73 ± 0.89[a])	12.23 ± 1.17
	Control 48 h	4.42 ± 0.38	54.87 ± 0.4	33.1 ± 1.1	4.42 ± 0.38
	5×10^{-5} M 48 h	4.97 ± 0.64	38.77 ± 2.62[a])	55.1 ± 3.1[a])	5.73 ± 0.57[a])
	1×10^{-6} M 48 h	5.20 ± 0.81	49.33 ± 1.02[a])	39.57 ± 2.17[a])	11.1 ± 1.78

[a]) Statistically significant at $p < 0.05$. The results are given in percentages of cells (% ± standard deviation) in a particular cell cycle phase.

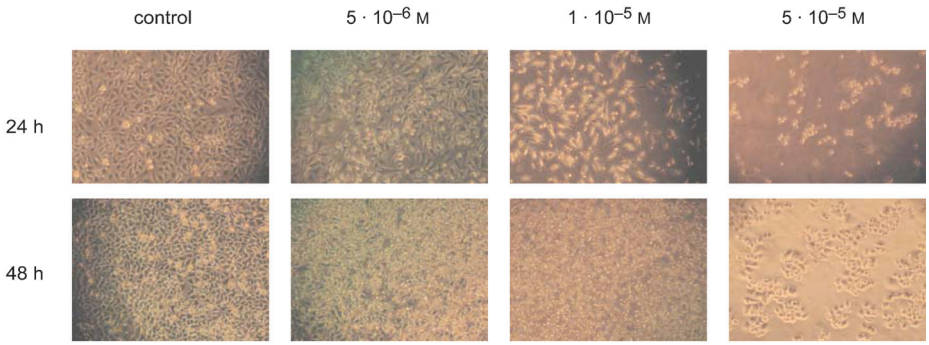

Fig. 6. *HeLa Cells treated with compound* **3** *after 24 h and 48 h treatment*

Observed morphological changes of HeLa cells treated with compound **3** are in line with cell-cycle analysis results (*Fig. 6*). Untreated HeLa cells formed an integrated confluent monolayer of large, flat cells. However, a change of cell morphology upon 24-h treatment that points to apoptosis (shrinkage of cells, chromatin condensation) has been induced with compound **3** at the highest tested concentration (5×10^{-5} M) which is in concordance with the cell-cycle analysis showing a rise in subG1 population under the same treatment condition. On the contrary, cells treated with lower concentrations (5×10^{-6} and 1×10^{-5} M) revealed a more spread appearance with widen cell–cell interspaces probably due to the cell-cycle arrest monitored by flow cytometry.

HeLa Cells on the other hand exerted strong apoptotic features upon the 48-h treatment at concentrations of 5×10^{-6} and 1×10^{-5} M confirmed by rise of subG1 population detected by flow cytometry as well. However, the highest tested concentration (5×10^{-5} M) induced formation of enlarged cells probably due to a strong S phase arrest. The damaged cells thus block the cell cycle, and if the damage is too high they ultimately die.

Conclusions. – Novel pyrimidine derivatives bearing isobutyl (in **3**, **4**, and **7**–**9**), and isobutenyl (in **5** and **10**) side chains at C(6), and dihydropyrrolo[1,2-*c*]pyrimidine-1,3-diones **6** and **11** were successfully synthesized and characterized. The position of the C=C bond in the side chains of compounds **3**–**5** and **7**–**10** depended on the nature or type of functionality used to protect the OH groups in the side chain. Thus, the Bn protecting groups gave rise to a C(2′)=C(3′) bond (compound **5**), whereas the Ac protecting groups led to a C(1′)=C(2′) bond (compound **10**). The dihydropyrrolo[1,2-*c*]pyrimidine-1,3-diones **6** and **11** were obtained as products of intramolecular cyclization, which occurred during the removal of the Bn (in **5**) or MeO protecting groups (in **10**).

Compounds **3**–**11** were shown to exert none or moderate antiproliferative effect on the tested tumor cell lines. However, 6-(1,3-dibenzyloxy)isobutyl-substituted 2,4-dimethoxypyrimidine derivative **3** showed the strongest concentration-dependent inhibitory activity against all tested cell lines similar to the effect of the control compound 5-FU. Furthermore, the results of the flow cytometric analysis revealed a strong influence of compound **3** on the cell cycle of HeLa cells. The mechanism of its

antiproliferative effect includes early increase of cells in G2/M phase, and apoptosis as well as the cell cycle arrest in the S phase upon prolonged treatment, accompanied with a concomitant decrease in G1 and subG1 cell populations. The increase of cells in the S phase after a prolonged treatment with compound **3** observed in our experiments might be a result of hampered DNA replication process due to a structural similarity of compound **3** with natural nucleosides. Besides, the pyrimidine derivative **5** with a C(2′)=C(3′) bond exhibited moderate non-specific cytostatic activity against HepG2, MCF-7, SW620, MiaPaCa-2, and WI38 cell lines at the highest tested concentration.

The biological results for **3** indicated that this compound is a lead compound for further synthetic structural optimization.

Support for this study was provided by the *Ministry of Science of the Republic of Croatia* (Projects No. 125-0982464-2925, No. 119-1193079-3069, No. 335-0982464-2393, and No 335-0000000-3532).

Experimental Part

1. *General*. M.p.: *Kofler* micro hot-stage (*Reichert*, Wien); uncorrected. TLC: Precoated *Merck* silica-gel *60 F-254* plates; detection of the spots under UV light (254 nm). Column chromatography (CC): silica gel (0.063–0.2 mm) *Fluka*; glass column slurry-packed under gravity. High-performance liquid chromatography (HPLC): *Agilent 1100* series system with UV detection (photodiode array detector) using *Zorbax* C_{18} reversed-phase (RP) anal. column (2.1 × 30 mm, 3.5 μM); all compounds used for biological evaluation showed >95% purity in this HPLC system. ^{1}H- and ^{13}C-NMR spectra: *Bruker 300* MHz NMR spectrometer; in (D_6)DMSO at 298 K, chemical shifts referenced to the residual solvent signal of DMSO at δ 2.50 ppm for ^{1}H and δ 39.50 ppm for ^{13}C; individual resonances were assigned on the basis of their chemical shifts, signal intensities, multiplicity of resonances and H,H coupling constants. MS: *Agilent 6410* instrument equipped with electrospray interface and triple quadrupole analyzer (LC/MS/MS).

2. *Synthesis*. 2.1. *1,3-Bis(benzyloxy)propan-2-one* (**2**) [26]. *N*-Chlorosuccinimide (NCS; 3.69 g, 0.27 mol) was suspended in dry CH_2Cl_2 (190 ml), and the mixture was cooled at −25° in a dry-ice bath. Me_2S (20.4 ml, 0.27 mol) was added under Ar. 1,3-Bis(benzyloxy)propan-2-ol (23 ml, 0.10 mol) in CH_2Cl_2 (100 ml) was added to the mixture, which was stirred at −25° for 2 h. Then, Et_3N (65.1 ml, 0.47 mol) was added, and the cooling bath was removed. The mixture was stirred overnight at r.t. and neutralized with 1M HCl. The org. layer was separated and washed with sat. aq. NaCl soln. (70 ml). The aq. layer was extracted with AcOEt (2 × 100 ml), and the org. layers were combined and dried ($MgSO_4$). After the removal of the solvents, the residue was purified using CC (hexane/AcOEt 4:1) to give **2** (18.0 g, 72.6%). Crude colorless oil. ^{1}H-NMR: 4.28 (*s*, CH_2(1), CH_2(3)); 4.52 (*s*, 2 PhCH_2O); 7.26–7.38 (*m*, 2 Ph). MS: 271.1 ([*M*+H]$^+$).

2.2. *1,3-Bis(benzyloxy)-2-[(2,6-dimethoxy-5-methylpyrimidin-4-yl)methyl]propan-2-ol* (**3**) [28]. LDA (28.64 ml, 2M in THF/heptane/ethylbenzene) was added dropwise to the soln. of **1** (4.81 g, 45 mmol) in THF (57 ml) at −70°. The temp. was raised to −55°, and the mixture was stirred for 30 min. To the mixture, the soln. of **2** (7.54 g, 28 mmol) in THF (41 ml) was added, and stirring was continued for 2.5 h at −55°. The soln. was neutralized with AcOH and evaporated. The oily residue was extracted with AcOEt and H_2O. The org. layer was dried ($MgSO_4$) and purified by CC (hexane/AcOEt 3:1 to afford **3** (4.4 g, 58.4%). M.p. 46–48°. ^{1}H-NMR: 2.03 (*s*, Me); 2.85 (*s*, CH_2(1′)); 3.33 (*s*, CH_2(3′), CH_2(3″)); 3.78 (*s*, MeO); 3.88 (*s*, MeO); 4.49 (*s*, 2 PhCH_2O); 5.10 (*s*, OH); 7.26–7.34 (*m*, 2 Ph). ^{13}C-NMR: 10.52 (Me); 37.84 (C(1′)); 54.37 (MeO); 54.42 (MeO); 72.98 (C(3′,3″)); 73.72 (PhCH_2O); 74.81 (C(2′)); 109.96 (C(5)); 127.76 (CH of Ph); 127.78 (CH of Ph); 128.60 (CH of Ph); 138.98 (C_q of Ph); 161.92 (C(6)); 165.94 (C(2)); 169.60 (C(4)). MS: 439.1 ([*M*+H]$^+$).

2.3. *4-[2-Fluoro-3-(phenylmethoxy)-2-[(phenylmethoxy)methyl]propyl]-2,6-dimethoxy-5-methylpyrimidine* (**4**) *and 2,4-Dimethoxy-5-methyl-6-[(2Z)-3-(phenylmethoxy)-2-[(phenylmethoxy)methyl]prop-2-en-1-yl]pyrimidine* (**5**). A soln. of **3** (3.23 g, 7.4 mmol) in dry CH_2Cl_2 (20 ml) was cooled to

$-78°$ and stirred for 15 min under Ar. DAST (7.5 mmol) was added dropwise, and the mixture was kept at $-78°$ for additional 15 min after which the cooling bath was removed. After 4 h of stirring at r.t., sat. aq. $NaHCO_3$ soln. (10 ml) was added, and the mixture was partitioned. The org. layer was separated, dried ($MgSO_4$), and evaporated to dryness. The raw product was purified by CC (hexane/AcOEt 3:1) to afford **4** (642 mg, 19.8%) as colorless and **5** (348 mg, 11.2%) as yellow oil.

Data of **4**. ^{1}H-NMR: 2.00 (*s*, Me); 3.11 (*d*, ^3J(H,F) = 18.1, CH_2(1′)); 3.65 (*dd*, ^2J(H,H) = 10.7, ^3J(H,F) = 22.8, CH_2(3′)); 3.72 (*s*, MeO); 3.81 (*d*, ^2J(H,H) = 10.8, ^3J(H,F) = 22.2, CH_2(3″)); 3.88 (*s*, MeO); 4.52 (*s*, 2 PhCH_2O); 7.26–7.38 (*m*, 2 Ph). ^{13}C-NMR: 10.45 (Me); 37.75 (*d*, *J*(C,F) = 23.1, C(1′)); 54.42 (MeO); 54.40 (MeO); 71.14 (*d*, *J*(C,F) = 24.3, C(3′,3″)); 73.08 (Ph*C*H_2O); 98.11 (*d*, *J*(C,F) = 177.4, C(2′)); 110.07 (C(5)); 127.92–128.88 (CH of Ph); 138.50 (C_q of Ph); 162.25 (C(2)); 163.48 (*d*, *J*(C,F) = 7.0, C(6)); 169.69 (C(4)). MS: 441.1 ($[M+H]^+$).

Data of **5**. ^{1}H-NMR: 1.94 (*s*, Me); 3.42 (*s*, CH_2(1′)); 3.75 (*s*, MeO); 3.81 (*s*, CH_2(3″)); 3.85 (*s*, MeO); 4.27 (*s*, PhCH_2O); 4.87 (*s*, PhCH_2O); 6.42 (*s*, H–C(3′)); 7.15–7.22 (*m*, Ph); 7.27–7.33 (*m*, Ph). ^{13}C-NMR: 10.05 (Me); 31.23 (C(1′)); 54.21 (MeO); 54.30 (MeO); 70.20 (C(3″)); 70.74 (Ph*C*H_2O); 73.65 (Ph*C*H_2O); 108.13 (C(5)); 111.12 (C(2′)) 127.67–129.29 (CH of Ph); 138.01 (C_q of Ph); 139.04 (C_q of Ph); 146.28 (C(3′)); 162.53 (C(6)); 167.39 (C(2)); 169.38 (C(4)). MS: 421.1 ($[M+H]^+$).

2.4. *2,4-Dimethoxy-5-methyl-6-{(2Z)-3-(phenylmethoxy)-2-[(phenylmethoxy)methyl]prop-2-en-1-yl}pyrimidine* (**5**). The mixture of **4** (642 mg, 1.46 mmol) and MeONa (395 mg, 7.3 mmol) in dry MeOH (20 ml) was heated to reflux for 3 d. The solvent was removed under reduced pressure, and the oily residue was extracted with CH_2Cl_2 and H_2O. The org. layer was dried ($MgSO_4$), and evaporation to dryness afforded **5** (464 mg, 75.6%) as yellow oil.

2.5. *6-(Chloromethyl)-4-methylpyrrolo[1,2-c]pyrimidine-1,3(2H,7H)-dione* (**6**). A mixture of **5** (205 mg, 0.5 mmol) in dry CH_2Cl_2 (10 ml) was cooled to $-78°$, and 1M BCl_3 soln. in CH_2Cl_2 (2 ml) was added under Ar. The mixture was stirred at $-78°$ for 2 h, then the temp. was raised to $-40°$, and the mixture was stirred for additional 2 h. The reaction was quenched by addition of CH_2Cl_2/MeOH 1:1 (5 ml), and the cooling bath was removed. The mixture was evaporated to dryness, and the crude product was purified by CC (CH_2Cl_2/MeOH 50:1) to give **6** (27 mg, 25.4%). Yellow crystals. M.p. >300°. ^{1}H-NMR: 1.86 (*s*, Me); 4.59 (*s*, CH_2Cl); 4.64 (*s*, CH_2(7)); 6.91 (*s*, H–C(5)); 11.11 (*s*, NH). ^{13}C-NMR: 10.33 (Me); 29.47 (CH_2Cl); 54.62 (C(7)); 103.61 (C(4)); 112.94 (C(6)); 121.30 (C(5)); 148.79 (C(6)); 150.32 (C(1)); 165.97 (C(3)). MS: 213.1 ($[M+H]^+$), 215.1 ($[M+H+2]^+$).

2.6. *2-[(2,6-Dimethoxy-5-methyl-4-pyrimidinyl)methyl]propane-1,2,3-triol* (**7**). A soln. of **3** (1.54 g, 3.52 mmol) in dry CH_2Cl_2 (40 ml) was cooled to $-78°$, and BCl_3 (1M in CH_2Cl_2, 14.1 ml) was added under Ar. The mixture was stirred at $-40°$ for 2 h, then CH_2Cl_2/MeOH 1:1 (70 ml) was added, and the cooling bath was removed. The solvents were evaporated under reduced pressure, and the residue was purified by CC (CH_2Cl_2/MeOH 10:1) to give **7** (639 mg, 70.4%). Yellow oil. ^{1}H-NMR: 2.07 (*s*, Me); 2.84 (*s*, CH_2(1′)); 3.28 (*d*, ^2J = 11.0, CH_2(3′)); 3.35 (*d*, ^2J = 11.0, CH_2(3″)); 3.95 (*s*, MeO); 3.98 (*s*, MeO); 4.48 (br. *s*, OH). ^{13}C-NMR: 10.52 (Me); 34.22 (C(1′)); 54.28 (MeO); 55.17 (MeO); 64.99 (C(3′,3″)); 76.00 (C(2′)); 107.02 (C(5)); 148.22 (C(6)); 150.73 (C(2)); 165.30 (C(4)). MS: 259.1 ($[M+H]^+$).

2.7. *2-[(2,6-Dimethoxy-5-methylpyrimidin-4-yl)methyl]-2-hydroxypropane-1,3-diyl Diacetate* (**8**). To the mixture of **7** (207.6 mg, 0.81 mmol), DMAP (15.5 mg, 0.12 mmol), and Et_3N (0.3 ml, 2.01 mmol) in dry MeCN (20 ml), Ac_2O (0.16 ml, 1.69 mmol) was added, and the mixture was stirred at r.t. for 40 min. The reaction was quenched with MeOH (1.3 ml), and the mixture was stirred for additional 5 min. After evaporation of volatile materials and CC (CH_2Cl_2/MeOH 10:1), **8** (163.4 mg, 54.3%) was isolated. Yellow oil. ^{1}H-NMR: 2.01 (*s*, 2 MeCO); 2.04 (*s*, Me); 2.87 (*s*, CH_2(1′)); 3.81 (*s*, MeO); 3.89 (*s*, MeO); 4.05 (*s*, CH_2(3′), CH_2(3″)); 5.38 (*s*, OH). ^{13}C-NMR: 10.60 (Me); 21.09 (*Me*CO); 37.98 (C(1′)); 54.42 (MeO); 66.65 (C(3′)); 72.67 (C(2′)); 110.24 (C(5)); 162.11 (C(6)); 164.68 (C(2)); 169.80 (C(4)); 170.57 (Me*C*O). MS: 343.1 ($[M+H]^+$).

2.8. *2-[(2,6-Dimethoxy-5-methylpyrimidin-4-yl)methyl]-2-fluoropropane-1,3-diyl Diacetate* (**9**). A soln. of **8** (348.5 mg, 0.93 mmol) in dry CH_2Cl_2 (40 ml) was cooled to $-78°$ and stirred for 15 min under Ar. DAST (1 mmol) was added dropwise, and the mixture was kept at $-40°$ for additional 2 h after which cooling bath was removed. To the mixture, MeOH (2 ml) was added, and stirring was continued for 15 min. The volatile materials were removed, and the residue was purified by CC (CH_2Cl_2/MeOH 40:1) to give **9** (90.8 mg, 26.0%). Colorless oil. ^{1}H-NMR: 2.04 (*s*, Me); 2.05 (*s*, 2 MeCO); 3.14 (*d*, ^3J(H,F) =

16.9, CH_2(1′)); 3.83 (*s*, MeO); 3.90 (*s*, MeO); 4.31 (*dd*, ^2J(H,H) = 12.4, ^3J(H,F) = 22.7, CH_2(3′)); 4.42 (*dd*, ^2J(H,H) = 12.2, ^3J(H,F) = 22.1, CH_2(3″)). ^{13}C-NMR: 9.89 (Me); 20.43 (*Me*CO); 35.77 (*d*, ^2J(C,F) = 23.4, C(1′)); 54.01 (MeO); 54.03 (MeO); 64.92 (*d*, ^3J(C,F) = 23.5, C(3′)); 95.14 (*d*, ^1J(C,F) = 179.9, C(2′)); 109.72 (C(5)); 161.85 (*d*, ^3J(C,F) = 7.8, C(6)); 169.40 (C(2)); 169.83 (C(4)); 170.20 (Me*C*O). MS: 345.1 ($[M+H]^+$).

2.9. *2-[(2,6-Dimethoxy-5-methylpyrimidin-4-yl)methylidene]propane-1,3-diol* (**10**). To a cold dry MeOH (10 ml), Na (28.2 mg, 1.21 mmol) was added, followed by compound **9** (91 mg, 0.24 mmol) dissolved in MeOH (2 ml). The mixture was refluxed for 1 h and became pale yellow. After removal of the solvent, the residue was purified using CC (CH_2Cl_2/MeOH 15 : 1) to give **10** (24.2 mg, 41.9%). White solid. M.p. 90–92°. ^{1}H-NMR: 2.03 (*s*, Me); 3.86 (*s*, MeO); 3.90 (*s*, MeO); 4.22 (*d*, ^2J = 4.3, CH_2(3′)); 4.43 (*d*, ^2J = 5.8, CH_2(3″)); 4.87 (*t*, ^3J = 5.9, OH); 5.06 (*t*, ^3J = 5.6, OH); 6.58 (*s*, H–C(1′)).^{13}C-NMR: 10.27 (Me); 54.40 (MeO); 54.54 (MeO); 59.45 (C(3′)); 62.97 (C(3″)); 107.94 (C(5)); 117.52 (C(1′)); 152.81 (C(2′)); 161.97 (C(6)); 162.36 (C(2)); 169.94 (C(4)). MS: 241.1 ($[M+H]^+$).

2.10. *6-(Hydroxymethyl)-4-methylpyrrolo[1,2-*c*]pyrimidine-1,3(2*H,7H*)-dione* (**11**). TMSCl (0.2 ml, 1.58 mmol) and NaI (82 mg, 0.54 mmol) were added under Ar to a stirred mixture of **10** (19 mg, 0.08 mmol) in dry MeCN (2 ml) at r.t. The mixture was stirred at 65° for 72 h, and the solvent was removed under reduced pressure. The residue was purified by CC (CH_2Cl_2/MeOH 10 : 1) to give **11** (10.4 mg, 67.1%). Oil. ^{1}H-NMR: 1.56 (*s*, Me); 3.93 (*s*, CH_2OH); 4.12 (*s*, CH_2(7)); 5.14 (*t*, ^3J = 5.4, OH); 6.18 (*s*, H–C(5)); 10.99 (NH). ^{13}C-NMR: 10.91 (Me); 58.51 (CH_2OH); 62.55 (C(7)); 105.80 (C(4)); 115.16 (C(6)); 145.70 (C(5)); 150.08 (C(4a)); 151.09 (C(1)); 165.27 (C(3)). MS: 195.1 ($[M+H]^+$).

3. *X-Ray Determination of Compounds* **3** *and* **6**[1]). Crystals suitable for X-ray single crystal study were grown from very dil. MeOH soln. for both compounds. The intensities were collected on an *Oxford Diffraction Xcalibur2* diffractometer with a *Sapphire 3 CCD* detector using graphite-monochromated MoK_α radiation (λ = 0.71073 Å) at different temps., 100 K for **3** and 295 K for **6**. The data collection and reduction were carried out with the *CrysAlis* programs [39]. The crystal structures were solved by direct methods [40]. All non-H-atoms were refined anisotropically by full-matrix least-squares calculations based on F^2 [40]. The H-atom attached to N(3) in **6** was found in a difference *Fourier* map, and its coordinates and isotropic thermal parameter have been refined freely. All other H-atoms in **3** and **6** were treated using appropriate riding models, with SHELXL97 defaults [40]. The choice of H-position of the OH group in both independent molecules of **3** was determined by best H-bond that could be created. Examination of the refined structure of **3** using ADDSYM option in PLATON [41] revealed possible additional symmetry, but the structure could not be refined satisfactorily in space group *Pbca*. In the absence of significant anomalous scattering, the *Flack* parameter was inconclusive, and the *Friedel* equivalents were, therefore, merged prior to the final refinement of this structure. PLATON program was used for analysis, and molecular and crystal structure drawings preparation [41].

Crystal Data of **3**. $C_{25}H_{30}N_2O_5$, M_r 438.51, orthorhombic space group $Pca2_1$; a = 24.9959(10), b = 17.1603(7), c = 10.7305(5) Å, V = 4602.7(3) Å^3; Z = 8; D_x = 1.266 g/cm^3; μ(MoK_α) = 0.088 mm^{-1}; S = 1.013; R/wR = 0.0692/0.1750 for 585 parameters and 3571 reflections with $I \geq 2\sigma(I)$, R/wR = 0.0844/0.1877 for all 4747 independent reflections measured in the range 7.92° – 2θ – 52.00°.

Crystal Data of **6**. $C_9H_9Cl_1N_2O_2$, M_r 212.63, monoclinic space group $P2_1/c$; a = 7.1834(2), b = 8.3351(3), c = 15.9522(5) Å, β = 98.681(3)°, V = 944.19(5) Å^3; Z = 4; D_x = 1.496 g/cm^3; μ(MoK_α) = 0.378 mm^{-1}; S = 1.043; R/wR = 0.0510/0.1583 for 132 parameters and 1576 reflections with $I \geq 2\sigma(I)$; R/wR = 0.0697/0.1674 for all 2271 independent reflections measured in the range 7.68° – 2θ – 56.00°.

4. *Antitumor Activity Assays.* 4.1. *Cell Culturing.* The cell lines HeLa (cervical carcinoma), SW620 (colorectal adenocarcinoma, metastatic), MiaPaCa-2 (pancreatic carcinoma), MCF-7 (breast epithelial adenocarcinoma, metastatic), HepG2 (hepatocellular carcinoma), and WI38 (normal human fibroblasts) were cultured as monolayers and maintained in *Dulbecco*'s modified *Eagle* medium (DMEM), supplemented with 10% fetal bovine serum (FBS), 2 mM L-glutamine, 100 U/ml penicillin, and 100 μg/ml streptomycin in a humidified atmosphere with 5% CO_2 at 37°.

---

[1]) CCDC-784295 and 784296 contain the supplementary crystallographic data for this article. These data can be obtained free of charge from the *Cambridge Crystallographic Data Centre via* www.ccdc.cam.ac.uk/data_request/cif.

4.2. *Proliferation Assays.* The panel cell lines were inoculated onto a series of standard 96-well microtiter plates on day 0, at 3000 to 6000 cells per well according to the doubling times of specific cell line. Test agents and the control compound 5-FU were then added in five- to tenfold dilutions (1×10^{-8} to 1×10^{-4} M) and incubated for further 72 h. Working dilutions were freshly prepared on the day of testing in the growth medium. The solvent (DMSO) was also tested for eventual inhibitory activity by adjusting its concentration to be the same as in the working concentrations (DMSO concentration never exceeded 0.1%). After 72 h of incubation, the cell growth rate was evaluated by performing the 3-(4,5-dimethylthiazol-2-yl)-2,5-diphenyl-2*H*-tetrazolium bromide (MTT) assay: experimentally determined absorbance values were transformed to a cell percentage growth (PG) using the formulas proposed by *NIH* and described in [42]. This method directly relies on control cells behaving normally at the day of assay, because it compares the growth of treated cells with the growth of untreated cells in control wells on the same plate – the results are, therefore, a percentile difference from the calculated expected value.

The IC_{50} and LC_{50} values for each compound were calculated from dose–response curves using linear regression analysis by fitting the mean test concentrations that give PG values above and below the reference value. If, however, all of the tested concentrations produce PGs exceeding the respective reference level of effect (*e.g.*, PG value of 50) for a given cell line, the highest tested concentration is assigned as the default value (in the screening data report, that default value is preceded by a '>' sign). Each test point was performed in quadruplicate in three individual experiments. The results were statistically analyzed (ANOVA, *Tukey* post-hoc test at $p < 0.05$). Finally, the effects of the tested substances were evaluated by plotting the mean percentage growth for each cell type in comparison to control on dose–response graphs.

4.3. *Cell-Cycle Analyses.* A total of 3×10^4 cells/well were seeded in a 6-well plate (*Falcon*, USA). After 24 h, HeLa cells were treated with the compound **3** at concentrations of 5×10^{-6}, 1×10^{-5}, and 5×10^{-5} M, and 5-FU at concentrations of 5×10^{-5} and 1×10^{-6} M. After 24 and 48 h, the attached cells were trypsinized, combined with floating cells, washed with PBS, and fixed with 70% EtOH. Immediately before the analysis, the cells were washed again with PBS and stained with 1 μg/ml of propidium iodide (PI) with the addition of 0.2 μg/ml of RNAse A. The stained cells were then analyzed with *Becton Dickinson FACScalibur* flow cytometer (10,000 counts were measured). Each test point was performed in triplicate. The percentage of the cells in each cell cycle phase was based on the obtained DNA histograms and determined using the WinMDI 2.9 and Cylchred software. Statistical analysis was performed in Microsoft Excel by using the ANOVA at $p < 0.05$.

REFERENCES

[1] C. Öğretir, M. Yaman, *J. Mol. Struct. (Theochem.)* **1999**, *458*, 217.
[2] M. Williams, E. A. Kowaluk, S. P. Arneric, *J. Med. Chem.* **1999**, *42*, 1481.
[3] C. Avendaño, J. C. Menéndez, 'Medicinal Chemistry of Anticancer Drugs', Elsevier, Amsterdam, 2008.
[4] T. Fojo, S. Bates, *Oncogene* **2003**, *22*, 7512.
[5] J. Nagata, H. Kijima, H. Hatanaka, S. Asai, H. Miyachi, A. Takagi, T. Miwa, T. Mine, H. Yamazaki, M. Nakamura, T. Kondo, K. J. Scanlon, Y. Ueyama, *Biochem. Biophys. Res. Commun.* ***2001****, 286*, 406.
[6] A. J. Oakley, M. Lo Bello, A. P. Mazzetti, G. Federici, M. W. Parker, *FEBS Lett.* **1997**, *419*, 32.
[7] C. Heidelberger, *Cancer Treat. Rep.* **1981**, *65*, 3.
[8] Y. Maehara, H. Kusumoto, H. Anal, T. Kusumoto, Y. Hiramoto, K. Sugimachi, *Eur. J. Cancer Clin. Oncol.* **1987**, *23*, 1511.
[9] K. Okabayashi, Y. Koyama, K. Maruyama, N. Okazaki, T. Sakano, T. Ise, *Jpn. J. Clin. Oncol.* **1979**, *9*, 35.
[10] J. Sigmond, G. J. Peters, *Nucleosides, Nucleotides Nucleic Acids* **2005**, *24*, 1997.
[11] A. V. Kadushkin, I. N. Nesterova, T. V. Golovko, I. S. Nikolaeva, T. V. Pushkina, A. N. Fomina, A. S. Sokolova, V. A. Chernov, V. G. Granik, *Pharm. Chem. J.* **1990**, *24*, 875.

[12] P. Das, C. P. Spears, A. H. Shahinian, S. K. Dasgupta, N. G. Kundu, *Bioorg. Med. Chem. Lett.* **1996**, *6*, 2477.
[13] M. Baba, E. De Clercq, H. Tanaka, M. Ubasawa, H. Takashima, K. Sekiya, I. Nitta, K. Umezu, R. T. Walker, S. Mori, *Mol. Pharmacol.* **1991**, *39*, 805.
[14] J. Balzarini, A. Karlsson, E. De Clercq, *Mol. Pharmacol.* **1993**, *44*, 694.
[15] A. Mai, M. Artico, G. Sbardella, S. Quartarone, S. Massa, A. G. Loi, A. De Montis, F. Scintu, M. Putzolu, P. La Colla, *J. Med. Chem.* **1997**, *40*, 1447.
[16] C. Heidelberger, 'Pyrimidine and Pyrimidine Antimetabolites', in 'Cancer Medicine', Eds. J. F. Holland, E. Frei, Lea and Febiger, Philadelphia, 1984, p. 8.
[17] N. G. Kundu, P. Das, J. Balzarini, E. De Clercq, *Bioorg. Med. Chem.* **1997**, *5*, 2011.
[18] N. G. Kundu. J. S. Mahanty, C. Chowdhury, S. K. Dasgupta, B. Das, C. P. Spears, J. Balzarini, E. De Clercq, *Eur. J. Med. Chem.* **1999**, *34*, 389.
[19] T. Gazivoda Kraljević, S. Krištafor, L. Šuman, M. Kralj, S. M. Ametamey, M. Cetina, S. Raić-Malić, *Bioorg. Med. Chem.* **2010**, *18*, 2704.
[20] S. Prekupec, D. Makuc, J. Plavec, S. Kraljević, M. Kralj, K. Pavelić, G. Andrei, R. Snoeck, J. Balzarini, E. De Clercq, S. Raić-Malić, M. Mintas, *Antiviral Chem. Chemother.* **2005**, *16*, 327.
[21] S. Krištafor, T. Gazivoda Kraljević, D. Makuc, J. Plavec, L. Šuman, M. Kralj, S. Raić-Malić, *Molecules* **2009**, *14*, 4866.
[22] S. Prekupec, D. Makuc, J. Plavec, L. Šuman, M. Kralj, K. Pavelić, J. Balzarini, E. De Clercq, M. Mintas, S. Raić-Malić, *J. Med. Chem.* **2007**, *50*, 3037.
[23] A. Johayem, S. Raić-Malić, K. Lazzati, P. A. Schubiger, L. Scapozza, S. M. Ametamey, *Chem. Biodiversity* **2006**, *3*, 274.
[24] C. Wurth, U. Kessler, J. Vogt, G. E. Schulz, G. Folkers, L. Scapozza, *Protein Sci.* **2001**, *10*, 63.
[25] S. Raić-Malić, A. Johayem, S. M. Ametamey, S. Batinac, E. De Clercq, G. Folkers, L. Scapozza, *Nucleosides, Nucleotides Nucleic Acids* **2004**, *23*, 1707.
[26] E. J. Corey, C. U. Kim, *J. Am. Chem. Soc.* **1972**, *94*, 7586.
[27] K. K. Ogilvie, N. Nguyen-Ba, R. G. Hamilton, *Can. J. Chem*. **1984**, *62*, 1622.
[28] L.-Y. Hsu, D. S. Wise, L. S. Kucera, J. C. Drach, L. B. Townsend, *J. Org. Chem.* **1992**, *57*, 3354.
[29] N. G. Kundu, B. Das, C. P. Spears, A. Majumdar, S. I. Kang, *J. Med. Chem.* **1990**, *33*, 1975.
[30] T. Gazivoda, S. Krištafor, M. Cetina, A. Nagl, S. Raić-Malić, *Struct. Chem.* **2008**, *19*, 441.
[31] S. Krištafor, T. Gazivoda, M. Cetina, D. Makuc, J. Plavec, S. Raić-Malić, *J. Mol. Struct.* **2009**, *923*, 19.
[32] J. Bernstein, R. E. Davis, L. Shimoni, N.-L. Chang, *Angew. Chem., Int. Ed.* **1995**, *34*, 1555.
[33] F. H. Allen, *Acta Crystallogr., Sect. A* **2002**, *58*, 380 (Version 5.31, May 2010).
[34] R. A. DeFilippis, E. C. Goodwin, L. Wu, D. DiMaio, *J. Virol.* **2003**, *77*, 1551.
[35] A. Cabelguenne, H. Blons, I. de Waziers, F. Carnot, A.-M. Houllier, T. Soussi, D. Brasnu, P. Beaune, O. Laccourreye, P. Laurent-Puig, *J. Clin. Oncol.* **2000**, *18*, 1465.
[36] S. Geisler, A.-L. Børresen-Dale, H. Johnsen, T. Aas, J. Geisler, L. A. Akslen, G. Anker, P. E. Lønning, *Clin. Cancer Res.* **2003**, *9*, 5582.
[37] S. Kraljević Pavelić, M. Marjanović, M. Poznić, M. Kralj, *J. Cancer Res. Clin.* **2009**, *135*, 1747.
[38] D. B. Lombard, K. F. Chua, R. Mostoslavsky, S. Franco, M. Gostissa, F. W. Alt, *Cell* **2005**, *120*, 497.
[39] Oxford Diffraction, Xcalibur CCD System, CrysAlis CCD and CrysAlis RED, *Oxford Diffraction Ltd.*, Abingdon, England, 2008.
[40] G. M. Sheldrick, *Acta Crystallogr., Sect. A.* **2008**, *64*, 112.
[41] A. L. Spek, *J. Appl. Crystallogr.* **2003**, *36*, 7.
[42] T. Gazivoda, S. Raić-Malić, V. Krištafor, D. Makuc, J. Plavec, S. Bratulić, S. Kraljević Pavelić, K. Pavelić, L. Naesens, G. Andrei, R. Snoeck, J. Balzarini, M. Mintas, *Bioorg. Med. Chem.* **2008**, *16*, 5624.

Received July 19, 2010